Control of Pharmaceutical Cocrystal Polymorphism on Various Scales by Mechanochemistry: Transfer from the Laboratory Batch to the Large-Scale Extrusion Processing

Tomislav Stolar,[†] Stipe Lukin,[†] Martina Tireli,[†] Irena Sović,[†] Bahar Karadeniz,[†] Irena Kereković,[‡] Gordana Matijašić,[§] Matija Gretić,[§] Zvonimir Katančić,[§] Igor Dejanović,[§] Marco di Michiel,[∥] Ivan Halasz,[†] and Krunoslav Užarević*,[†]

[†]Division of Physical Chemistry, Ruđer Bošković Institute, Bijenička cesta 54, 10000 Zagreb, Croatia

[‡]University of Applied Health Sciences, Mlinarska cesta 38, HR-10000 Zagreb, Croatia

[§]University of Zagreb, Faculty of Chemical Engineering and Technology, Trg Marka Marulića 19, 10000 Zagreb, Croatia

[∥]ESRF—European Synchrotron Radiation Facility, 71 Avenue de Martyrs, 38000 Grenoble, France

Supporting Information

ABSTRACT: We demonstrate a controllable mechanochemical synthesis of cocrystal polymorphs of ascorbic acid (vitamin C) and nicotinamide (vitamin B3) on different scales and without using bulk solvents. Next to the previously described polymorph of the 1:1 cocrystal, which is one of the first cocrystals approved for human consumption, we report here a new, thermodynamically more stable polymorph detected during in situ synchrotron powder X-ray diffraction monitoring of milling reactions. The new polymorph is currently available exclusively by mechanochemical synthesis, and its crystal structure was determined from synchrotron powder X-ray diffraction data. Laboratory in situ monitoring by Raman spectroscopy provided direct insight into the cocrystals formation and was further used to optimize the manufacturing procedure. Subgram synthesis using a laboratory mixer mill was transferred to the 10 g scale on a planetary ball mill and continuous manufacturing using a twin-screw extruder. Both cocrystal polymorphs perform excellently in tableting, thus alleviating the notoriously poor compactible properties of vitamin C, while the mechanochemical cocrystallization does not harm its antioxidant properties.

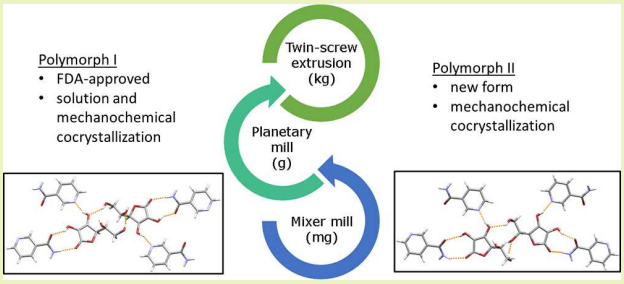

KEYWORDS: *Mechanochemistry, Active pharmaceutical ingredients, Polymorphism control, Large-scale processing, Twin-screw extrusion*

INTRODUCTION

The use of mechanochemistry in modern materials chemistry continues to grow because of its efficiency, selectivity, and ecological suitability in obtaining the desired products.[1−4] Those characteristics go along with the increasing need to create more sustainable drug manufacturing processes, as has been stressed recently by the consortium of pharmaceutical companies.[5] Mechanochemistry in the pharmaceutical industry is primarily used as a screening technique for solid forms of polymorphs, salts, and cocrystals of active pharmaceutical ingredients (APIs),[6−9] but its role in the synthesis of APIs is becoming increasingly important.[10−12] One way of transferring laboratory-scale mechanochemical production to larger manufacturing scales is utilizing twin-screw extrusion (TSE).[13] TSE process is based on adding the reaction mixture through the feeder at one end, and two corotating screws are used for mixing, shearing, and conveying of the material that exits on the other end. TSE is used for the continuous production of a variety of chemicals, such as organics,[14−16] metal−organic frameworks (MOFs),[17,18] organic light-emitting diode (OLED) materials,[19] and cocrystals.[20−22]

Cocrystallization is a convenient way of improving chemical and physical stability,[23−25] compressibility[26] and bioavailability[27−30] of APIs. More than a decade of extensive research in the area of pharmaceutical cocrystals has shown that they offer enhanced API properties and more diverse space of solid forms for APIs that lack ionizable functional groups, which is a requirement for salt formation.[31] Despite apparent advantages cocrystals may offer, their appearance on the market is still very scarce,[32] which is mainly up to their previous regulatory classification as well as manufacturing scale-up concerns.[33] Latest US Food and Drug Administration (FDA) guidance for pharmaceutical industry states that from a regulatory perspective, a cocrystal of API and suitable coformer is

considered analogous to a new polymorph of API.[34] That means that API cocrystal is now in the same class as API polymorphs and salts. The expectations are that there will be a significant increase in API cocrystals becoming available on the market as evidenced by the recent commercialization of sacubitril–valsartan cocrystal drug by Novartis, branded as Entresto, to treat chronic heart failure.[35]

Vitamin C is common in pharmaceutical and food supplements industry and has the largest production among all vitamins, estimating 110 kilotons per year.[36] One of the first cocrystals approved for human consumption by the FDA (21CFR172.315) is cocrystal of vitamin C (L-(+)-ascorbic acid, **asc**) and nicotinamide (a form of vitamin B3, **na**) as a formulation for inclusion into multivitamin preparations.[37] It is known for this cocrystal (from now on **I**, Figure 1) to have

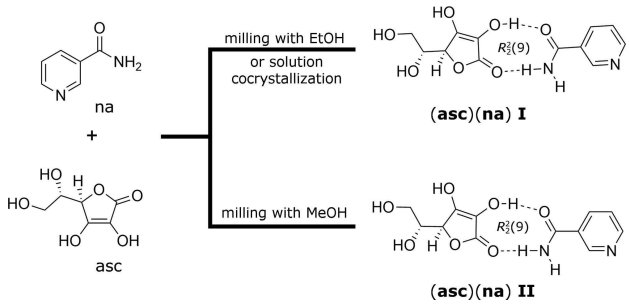

Figure 1. Molecular structures of nicotinamide (form of vitamin B3) and L-(+)-ascorbic acid (vitamin C) and the reaction conditions for the preparation of two polymorphs of (**asc**)(**na**) cocrystal.

antiscorbutic properties (prevention of scurvy) and certain activity against tuberculosis.[38,39] It was recognized in the 1940s, when in an attempt to prepare capsule of vitamin C with nicotinamide, authors observed its anomalous behavior and change of the reaction mixture color to yellow.[40] Further study revealed that nicotinamide and vitamin C are forming 1:1 "addition compound," either by crystallization from ethanol (EtOH) or by mechanical mixing and latter was patented by Gelatin Products Corporation.[41] In 1949, Wenner[42] identified this compound to be a molecular complex, not salt, which was confirmed almost 70 years later, after solving the structure of **I** in 2016.[43]

Here, we report extensive research on the transfer of mechanochemical cocrystallization procedures to various scales, demonstrated on the reaction between **asc** and **na** (Figure 1). We used recently developed in situ monitoring of mechanochemical transformations[44] by synchrotron powder X-ray diffraction (PXRD),[45−53] to detect the existence of a new, thermodynamically more stable cocrystal polymorph (**asc**)(**na**) **II**(from now on **II**, Figure 1). Laboratory monitoring of milling reactions using in situ Raman spectroscopy[54] was further used to optimize the production procedures. For larger scales, we aimed to selectively prepare both cocrystal polymorphs on a 10 g scale via planetary ball milling and also to transfer these batch processes into a continuous TSE process on the industrial scale (~1 kg/hour rate). We solved the crystal structure of **II** from PXRD data and the slurry competition experiments were used to establish the thermodynamic relationship with **I**. The direct tableting of cocrystal polymorphs prepared in the solid-state was assessed to try to account for poor tableting properties of vitamin C.[55−58]

■ EXPERIMENTAL SECTION

Chemicals and Solutions. L-(+)-ascorbic acid 99+% and nicotinamide 99% were purchased from Alfa-Aesar and used as received. For liquid-assisted grinding (LAG) experiments we used p.a. methanol (MeOH) and p.a. EtOH from Kemika. ABTS ((2,2′-azinobis(3-ethylbenzothiazoline-6-sulfonic acid)) was purchased from Sigma-Aldrich. 5 mM solution of ABTS was prepared in 0.1 M phosphate buffer, pH = 7.4. Trolox (6-hydroxy-2,5,7,8-tetramethychroman-2-carboxylic acid) was purchased from Sigma-Aldrich. A 5 mM solution of Trolox was prepared in ethanol. Phosphate buffer (0.1 M), pH = 7.4, was prepared from disodium phosphate dihydrate and monosodium phosphate dihydrate purchased from Kemika. Potassium peroxydisulfate was purchased from Merck and 65 mM solution was used. 5 mM EtOH solutions of **I** (mechanochemical synthesis), **II** (mechanochemical synthesis), **I** (isolated from EtOH solution), L-(+)-ascorbic acid, nicotinamide, and mixture of L-(+)-ascorbic acid and nicotinamide were prepared in p.a. EtOH. All the chemicals were of analytical grade, and all solutions were prepared with ultrapure water from Millipore Milli-Q system (Milli-Q, USA) if not stated otherwise.

Cocrystallization Experiments. Mechanochemical cocrystallization experiments by IST500 mixer mill (InSolido Technologies) were performed in 14 mL of poly(methyl methacrylate) (PMMA) jars using the same reaction conditions: 250 mg overall mass of reactants in 1:1 stoichiometric ratio (0.838 mmol of **asc** and 0.838 mmol of **na**), 20 μL of appropriate liquid additive (if not stated otherwise), two stainless steel balls of 7 mm diameter as grinding media (each weighing 1.42 g), 30 Hz grinding frequency, and 60 min grinding time. Solution cocrystallization experiments were done by dissolving 50 mg of a solid mixture containing nicotinamide and L-(+)-ascorbic acid in 1:1 stoichiometric ratio (0.168 mmol of **asc** and 0.168 mmol of **na**) in 0.5−1 mL of appropriate solvent.

Ten Gram Scale by Planetary Ball Milling. Planetary ball milling was performed by mixing 5.9 g of vitamin C and 4.1 g of nicotinamide in a 50 mL zirconia jar. EtOH (0.8 mL) or MeOH (1.6 mL) was added as the liquid additive, and four 10 mm zirconia balls were used as milling media. Reaction time was 60 min at 400 rpm.

Twin-Screw Extrusion. The continuous mechanochemical synthesis was carried out in Rondol 21 mm LAB TWIN corotating, intermeshing twin-screw extruder (TSE). All contact points were made of stainless steel. Total barrel length was 630 mm, leading to L/D ratio of 30. Apart from forward-conveying sections, screws were equipped with three kneading blocks comprising 5 mm wide bilobed elements arranged in 30°, 60°, and 90° stagger angles with lengths of 65, 25, and 50 mm, respectively. The barrel of the extruder consisted of five individual heating/cooling sections and was kept at 40 °C to ensure smooth screw rotation. For the purpose of this experiment, the die at the end of the extruder barrel was removed, and the extruded material was collected in a weighed beaker. Reactants were gently premixed in a beaker and fed manually through the first feed port. The screw speed was kept at 180 rpm, at which torque was kept at 90% of the maximum value, providing as high as possible throughput for the current screw configuration. To facilitate longer residence times and ensure higher conversion, the obtained product was fed through the extruder one more time.

Preparation of ABTS$^{\bullet+}$. The ABTS$^{\bullet+}$ solution was prepared 24 h before spectroscopic measurement by mixing 0.5 mL of 65 mM $K_2S_2O_8$ and 25 mL of 5 mM ABTS prepared in 0.1 M phosphate buffer, pH 7.4.[59] The mixture was left in the dark at room temperature. For this study, the ABTS$^{\bullet+}$ solution was diluted with 0.1 M phosphate buffer, pH 7.4, to an absorbance of 0.739 ± 0.02 at 734 nm. ABTS$^{\bullet+}$ is stable radical (radical was stable for more than 2 days when stored in the dark at room temperature).

Measurement of Antioxidant Activity. One milliliter of the ABTS$^{\bullet+}$ solution was placed in 1.5 mL spectroscopic cuvette. After a steady state of absorbance (cca 1 min) was reached, 5 μL of measured sample, Trolox standard, or antioxidant solutions was added to the cuvette and mixed for 5 s. The changes in absorbance were read after 1 and 4 min. All determinations were carried out in triplicate.

Characterization. X-ray powder diffraction data was collected on PANalytical Aeris diffractometer with Ni-filtered CuK radiation, and with the X-ray tube operating at 7.5 mA and 40 kV. Fourier-transform infrared attenuated total reflectance (FTIR-ATR) spectra were recorded on PerkinElmer SpectrumTwo spectrometer equipped with a diamond cell in the range of 4000−450 cm^{-1} and with a resolution of 4 cm^{-1}.

Particle Size Distribution. The particle size distribution was obtained using laser diffraction analyzer SALD-3101 (Shimadzu, Japan) with measuring range from 0.3 to 3000 μm. Dry measuring unit was used and the samples were dispersed at 0.4 MPa. Presented particle size distribution is a mean value of three measurements.

Tableting. For the tableting process, 10 g of **I** and **II** obtained by planetary ball milling was used. Compression was performed using an eccentric single punch tableting machine TDP-5T (Zhejiang Wisely Machinery Co. Ltd., China) equipped with 8 mm round punches. All tablets were produced using equal compression force and 5 mm charging depth.

Surface Characterization of Tablets. Surface morphology of prepared tablets was examined using stereomicroscope SZX 16 (Olympus, Japan) at magnifications of 25×.

In Situ Monitoring. PXRD monitoring of the milling reactions was performed in amorphous PMMA jars with two stainless steel balls as milling media at the European Synchrotron Radiation Facility (ESRF) in Grenoble, France, at ID15A beamline. For reactions, we used remotely operated IST500 (InSolido Technologies) mixer mill produced for this kind of measurements and operated at 30 Hz. Beam energy was set to 69 keV (λ = 0.1797 Å) to achieve the best possible resolution between diffraction peaks. X-ray beam was set to pass through the bottom of the jar and exposure time for each pattern was 5 s. Diffraction data were recorded on a Dectris Pilatus CdTe 2 M detector positioned 730 mm from the sample, radial integration of the raw diffraction images was performed with an in-house Matlab script. Experimental hutch was air conditioned to 21 °C. Laboratory in situ Raman spectroscopy was performed in the same experimental conditions using portable Raman system with OceanOptics Maya2000Pro spectrometer coupled with PD-LD (now Necsel) BlueBox laser source (λ = 785 nm) with B&W-Tek fiber optic Raman BAC102 probe. Raman probe was positioned ∼1 cm from the bottom of the jar and Raman spectra were collected as described previously.[60]

Analysis of Raman Spectra. First, PMMA jar contribution was subtracted from each spectrum, and remaining spectra were baseline corrected and normalized with the Euclidian norm. Details of the procedure can be found elsewhere.[60] Spectra were arranged in a data matrix and subjected to the multivariate curve resolution−alternative least-squares (MCR-ALS) procedure to extract spectral and concentration profiles.[61] Additional constraints, like closure and non-negativity in spectral and concentrations spectral contributions were used to obtain physically meaningful results.[62] Additionally, spectra of pure components from the MCR-ALS procedure were compared to the actual Raman spectra of reactants, **I** and **II**. The spectrum of the unknown intermediate phase from MCR-ALS could not be obtained in pure form since it also contains the contributions from the reactants, **I** and **II**.

Crystallographic Section. Powder diffraction data for the crystal structure solution of **II** was collected in a capillary on a high-resolution powder diffractometer at the 11-BM beamline of the Advanced Photon Source, Argonne National Laboratory, IL, USA, with a radiation wavelength of 0.457705 Å. The structure was solved by simulated annealing in direct space taking advantage of known molecular fragments of L-(+)-ascorbic acid and nicotinamide which were treated independently as rigid bodies. Structure solution was recognized after meaningful networks of hydrogen bonding were formed. Structure refinement was finally performed on atoms using geometry restraints on bond distances and angles as well as planarity restraints on nicotinamide molecule. All calculations were performed using the program Topas. The CIF file, also containing the measured and calculated diffraction patterns, has been deposited with the Cambridge Crystallographic Data Centre (CCDC) under the deposition number 1883265. These data can be obtained from the CCDC upon request.

RESULTS AND DISCUSSION

In Situ Mechanochemical Reaction Monitoring. We aimed to develop a mechanochemical procedure for the production of (**asc**)(**na**) cocrystal, both on the laboratory and multigram scale. As the mechanochemical reactivity significantly increases by the addition of liquids in liquid-assisted grinding (LAG),[63−65] we tested several liquids as additives for milling reactions (Table S1 and Figure S1). Monitoring of the mechanochemical reaction between **asc** and **na** using 20 μL of EtOH as the liquid additive revealed fast consumption of reactants and almost immediate occurrence of an intermediate, short-lived phase which was not possible to isolate as it occurs concomitantly with reactants and lives for ∼15 min. The formation of known phase **I** (Figures 2 and 4a, 4c) started after 5 min and finished after 25 min of milling. We isolated **I** as the final product after 60 min of milling.

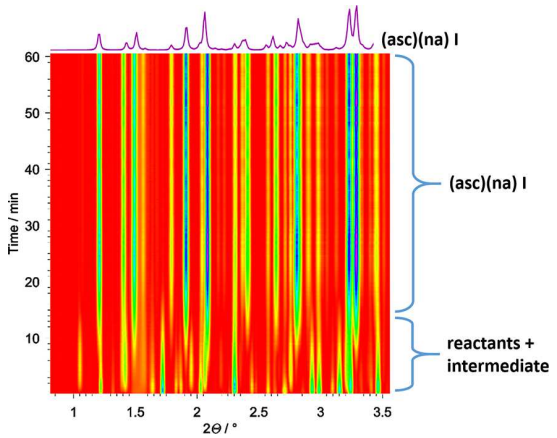

Figure 2. Time-resolved X-ray powder diffraction patterns of in situ monitoring of milling 1:1 reaction mixture of vitamin C and nicotinamide using ethanol as the liquid additive. Color code: Blue, high intensity; red, low intensity.

Switching to MeOH additive induced a change in the reaction pathway. Milling the reaction mixture of **asc** and **na** with 20 μL of MeOH revealed the fast occurrence of the same intermediate phase that lived concomitantly with reactants for approximately 3 min. Formation of **I** is finished after 9 min of milling. Further milling resulted in the occurrence of a new phase, **II**, which started to form after 20 min and with the simultaneous diminishing of diffraction peaks of **I** (Figure 3). However, subsequent analysis of the final pattern collected after 90 min of milling revealed that the final product is a mixture of **I** and **II** (Figure S12).

Intermediate that can be seen in LAG with EtOH and MeOH does not appear in neat grinding (Figure S3). Therefore, it seems that its formation is favored only in LAG conditions.

To obtain only **II**, we increased the volume of added MeOH to 40 μL since the liquid additive volume can have a substantial effect on the reaction outcome.[66,67] In situ Raman monitoring of LAG reaction with 40 μL of MeOH revealed much faster cocrystallization. Form **I**, which formed in first 10 min of milling, transformed to **II** as observed in LAG with 20 μL of MeOH, but this time the transformation was completed after

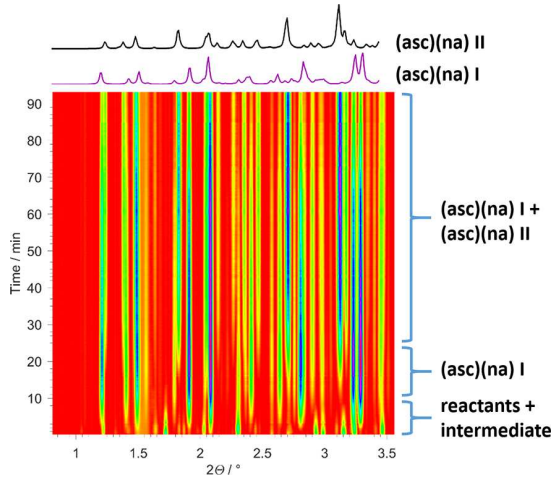

Figure 3. Time-resolved X-ray powder diffraction patterns of in situ monitoring of milling 1:1 reaction mixture of vitamin C and nicotinamide using methanol as the liquid additive. Color code: blue, high intensity; red, low intensity.

40 min of milling (Figures 4b and 4d). The final product was pure solid phase **II**, with FTIR-ATR and Raman spectrum similar to **I** (Figures S10 and S11).

Crystal Structure Studies. Crystal structure of **II** was solved from PXRD data (Figure 5) with crystallographic parameters as given in Table 1.

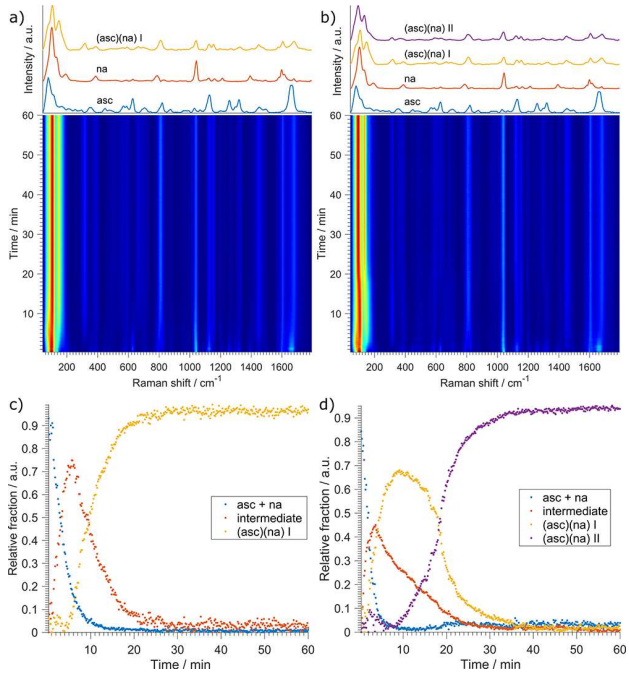

Figure 4. Time-resolved Raman spectra of in situ monitoring of milling 1:1 reaction mixture of vitamin C and nicotinamide using (a) ethanol and (b) methanol as the liquid additives. Color code: red, high intensity; blue, low intensity. Reaction profiles extracted with multivariate curve resolution alternative least-squares procedure from Raman monitoring of milling 1:1 reaction mixture of vitamin C and nicotinamide using (c) ethanol and (d) methanol as the liquid additives.

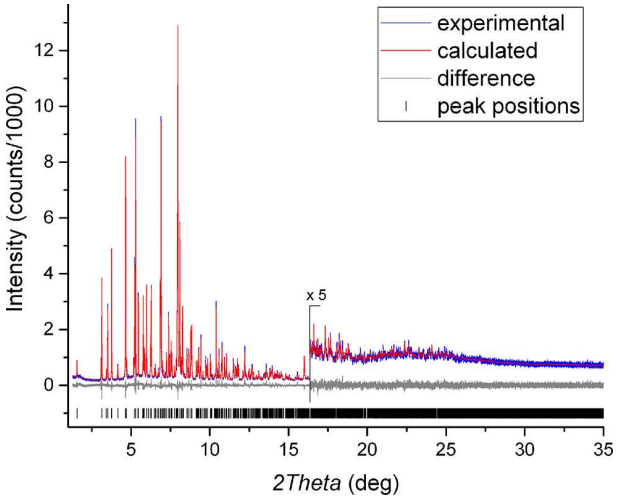

Figure 5. Rietveld fit for the refinement of the crystal structure of **II**. The high-angle region of the pattern is enlarged to reveal more detail. Radiation wavelength is 0.457705 Å.

Table 1. Crystallographic Data for II

molecular formula	$C_{12}H_{14}N_2O_7$
formula weight (g mol^{-1})	298.28
space group	$P2_1$
a (Å)	7.749926 (33)
b (Å)	33.38721 (15)
c (Å)	5.081955 (22)
α (deg)	90
β (deg)	99.13411 (28)
γ (deg)	90
V (Å^3)	1298.2735 (99)
Z	4
temperature (K)	298
radiation type	synchrotron
wavelength (Å)	0.457705
R_p	0.049
R_{wp}	0.062
GOF	1.17
$R(F^2)$	0.022

Both polymorphs crystallize in chiral space groups, **I** in the triclinic $P1$ and **II** in the monoclinic $P2_1$ space group. Asymmetric units of both polymorphs contain two molecules of **asc** and **na**. They both exhibit very similar intermolecular and crystal packing interactions characterized by chains of hydrogen bonding interactions and by a ring $R_2^2(9)$ heterosynthon in which one −OH group of **asc** forms a hydrogen bond with the C═O group of **na**, while the C═O group of **asc** forms a hydrogen bond with the $-NH_2$ group of **na**(Figure 6a and 6b).[68] Network of hydrogen bonds further assembles into layers (Figure 6c and 6d).

Solution Screening and Relative Stability Measurements. After obtaining two polymorphs mechanochemically, for comparison, we also performed solution cocrystallization. We dissolved mixtures containing **asc** and **na** in different solvents (Table S2 and Figure S1) allowing for full solvent evaporation, and isolated yellow precipitates. As evidenced from the PXRD data, solution cocrystallizations resulted exclusively in **I**, even when the bulk solvent was MeOH, which is in agreement with the literature.[69] As opposed to LAG

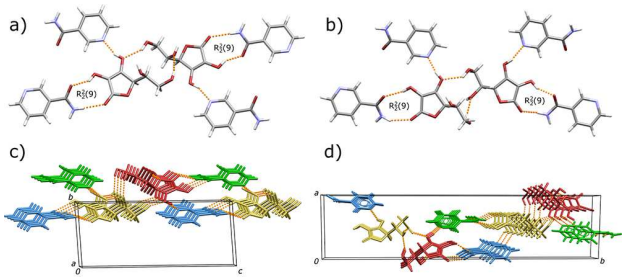

Figure 6. Hydrogen bonding motives in (a) **I** and (b) **II**. Both structures exhibit similar hydrogen bonding interactions and are stabilized by $R_2^2(9)$ supramolecular synthon between **asc** and **na** molecules. Hydrogen bonded networks form layers in (c) **I** and (d) **II**.

experiments, where the addition of water resulted in the formation of pure **II** (Figure S1) but with nonhomogeneous distribution of milled solid (Figures S2 and S4), attempt to crystallize product from water resulted only in brown glutinous solution which darkened over time, without any crystals occurrence.

The thermodynamic relationship between polymorphs was determined in the slurry experiments in acetonitrile, in which both polymorphs have low solubility, and at room temperature. Equal amounts of both polymorphs were stirred in acetonitrile for 24 h, after which the solid in the slurry was carefully isolated and dried in air. PXRD data revealed that the dried sample was pure **II**, revealing the complete transformation of **I** to a more thermodynamically stable **II** (Figure S6). Results from the slurry experiments are in agreement with Ostwald's rules of stages:[70] less thermodynamically stable **I** appears first and then transforms to **II** upon continued milling (Figure 4d). Both polymorphs are however bench-stable for at least six months (Figure S7).

Scaling up Manufacturing Processes for Both Cocrystal Polymorphs. Scaling up mechanosynthesis of both polymorphs to 10 g has been achieved with the planetary mill. We used TSE for solid-state flow synthesis on a 100 g test scale. For 10 g scale, we used Fritsch Pulverisette 6 planetary mill operating at 400 rpm, and zirconia milling equipment to avoid pollution of products. Transfer of mixer mill to planetary mill synthesis was successful for both polymorphs, and both MeOH and EtOH additives resulted in the quantitative formation of target polymorph form after 60 min of milling (Figure S8).

For TSE experiments, we used Rondol 21 mm LAB TWIN extruder with 630 mm long barrel and five individual heating sections (Figure 7). We premixed **asc** and **na** in a glass beaker before started to adding it carefully through the feeder, and 40 mL of EtOH or MeOH were added through the adjacent inlet for approximately 110 g of the reaction mixture. As a standard TSE procedure, the obtained mixture was fed through the extruder one more time to ensure the better transformation of reactants to the desired product. In the same manner as on the laboratory scale, selective synthesis and polymorphism could be controlled even during the continuous manufacturing process (Figure S9). Rietveld analysis of the extrusion products showed some excess of reactants in case of **I** (Figure S13), whereas we obtained phase pure **II** (Figure S14). At the screw speed of 180 rpm, the accomplished throughput was in the range of 21−23 g/min for each extrusion cycle. As for the space-time yield (STY) for these three different reactors, mixer mill provided the lowest STY of 440 kg m^{-3} d^{-1}, whereas the

Figure 7. Twin-screw extruder used for the continuous synthesis of (**asc**)(**na**) polymorphs. All contact points are made of stainless steel.

use of planetary mill significantly increased the STY to 4800 kg m^{-3} d^{-1}. In accordance with recent reports,[13−15] continuous processing by TSE resulted in orders of magnitude increase in STY, amounting to ∼324 400 kg m^{-3} d^{-1}.

Antioxidant Activity of Prepared Cocrystal Polymorphs. To test the effect of the mechanical action on the activity and quality of vitamin C, we performed TEAC assay (Trolox equivalent antioxidant capacity), a standard test for estimation of activity of vitamin C, which was first reported by N. J. Miller et al.[71] and later improved.[72] TEAC is a measurement of antioxidant strength based on Trolox (6-hydroxy-2,5,7,8-tetramethychroman-2-carboxylic acid) and expressed in Trolox Equivalents, estimated from the loss of color when antioxidant is added to the blue-green chromophore ABTS ((2,2′-azinobis(3-ethylbenzothiazoline-6-sulfonic acid)) radical cation ($ABTS^{\bullet+}$). The antioxidant reduces $ABTS^{\bullet+}$ to ABTS causing decolorization (Figure S18). The Trolox equivalents were calculated by dividing the difference in absorbance of the sample ($\Delta A = A(ABTS^{\bullet+})$-A(sample)) with the difference in absorbance of the Trolox ($\Delta A = A(ABTS^{\bullet+})$-A(Trolox)).

For all measurements, 5 mmol solutions were used. After 1 min, pure L-(+)-ascorbic acid demonstrated the Trolox equivalent of 0.964 ± 0.096 (mean of three determinations ± standard deviation.), that is, antioxidant activity is substantial as expected (Table 2). The nicotinamide demonstrated the low Trolox equivalent of 0.005 ± 0.003, revealing low antioxidant activity. **I** and **II** obtained by

Table 2. Trolox Equivalents after 1 and 4 min for L-(+)-Ascorbic Acid, Nicotinamide, I (Planetary Ball Milling), II (Planetary Ball Milling), I (Solution Synthesis), and the Mixture of L-(+)-Ascorbic Acid and Nicotinamide

sample	Trolox equivalent	
	1 min	4 min
asc	0.964 ± 0.096	0.965 ± 0.089
na	0.005 ± 0.003	0.009 ± 0.005
I-mech	0.481 ± 0.050	0.482 ± 0.050
II-mech	0.438 ± 0.009	0.440 ± 0.008
I-solution	0.485 ± 0.048	0.486 ± 0.048
asc and **na** (1:1) mixture	0.508 ± 0.045	0.510 ± 0.050

planetary ball milling displayed similar Trolox equivalents compared to **I** obtained from solution, amounting to 0.481 ± 0.050, 0.438 ± 0.009, and 0.485 ± 0.048, respectively. This activity, stemming from the lower quantity of vitamin C in cocrystal is similar to the blind probe solution, containing vitamin C and nicotinamide in similar quantities, which demonstrated the Trolox equivalent of 0.508 ± 0.045. After 4 min, the antioxidant activity of all samples was not significantly higher when compared to the one observed after 1 min, which indicates fast reaction kinetics. These results confirm that the proposed milling procedures do not harm the antioxidant activity of vitamin C.

Mechanical Properties and Particle Size Distribution of Cocrystal Polymorphs. Both (**asc**)(**na**) cocrystal polymorphs prepared on a 10 g scale in a planetary ball mill were tested for their compressibility in the tableting process without any additional particle size reduction. Before measurement and tableting, samples were separated using 1 mm sieve to remove larger chips of the material. Initially, we compared the particle size distribution of reactants, **asc** and **na** to obtained cocrystal polymorphs (Figures S15−S17). Pure **asc** has a very broad particle size distribution (0.3−1000 μm), and most of the particles are in the range from 30 to 1000 μm, while **na** particles are in the range from 10 to 200 μm. Both initial samples have very poor flowability and compressibility, and it was not possible to obtain their tablets by direct tableting, as they clogged the tableting machine. Wide size distribution is preferable in tableting and results in better packaging of particles and tablet strength. Smaller particles have a dual role, filling the voids between particles and also act as glidant by sticking to the surface of bigger particles and improving powder flowability.[73] Samples from extrusion are also characterized by a large ratio of big particles and large flakes, and these samples were unsuitable for tableting assessment without additional mechanical treatment. On the other hand, cocrystal polymorphs obtained from planetary ball mill displayed excellent flowability and compressibility. Both samples have a high content of smaller particles (<10 μm), and similar particle size distribution (Figures S15 and S16). As evidenced from tablet stereomicrographs, tablets of both cocrystal polymorphs have a smooth surface (Figure 8a and 8b). Both samples were compressed at 5 mm charging depth, but depending on the compressibility of the powder, different thickness and hardness were obtained with **II** having slightly better compressibility (Figure 8c and 8d). After tableting, both **I** and **II** retained their respective solid forms (Figure S19). It can be concluded that both polymorph samples were suitable for direct compression. However, to achieve better quality of the tablets, additional pulverization of the products or the addition of some excipients may be necessary. Molecular sheets that further form layers, which can be found in crystal structures of both **I** and **II** (Figure 6c and 6d), resemble the crystal packing in orthorhombic polymorph of paracetamol.[74] It was shown how these layers contribute to better compression behavior making orthorhombic polymorph of paracetamol suitable for direct tableting process as well.[75]

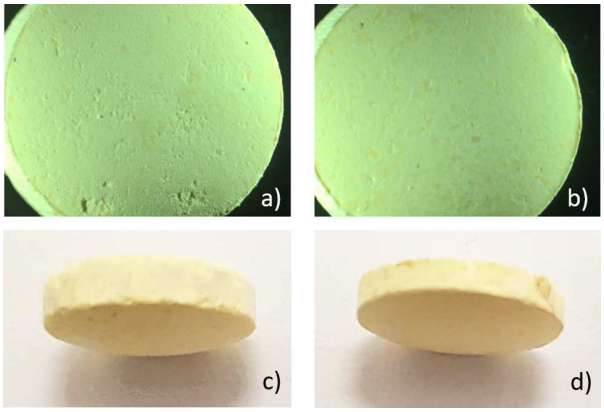

Figure 8. Surface of the tablets prepared by direct tableting of (a) **I**-planetary and (b) **II**-planetary and thickness of the tablets of (c) **I**-planetary and (d) **II**-planetary. All samples were compressed as received without additional mechanical treatment.

CONCLUSION

We demonstrated here how mechanochemistry enables fast, controllable, and scalable synthesis of polymorphic cocrystals, shown on an FDA-approved pharmaceutical cocrystal of vitamin C and nicotinamide. State-of-the-art in situ monitoring of milling reactions was used here to detect and capture new polymorph **II**, thermodynamically more stable when compared to the known form **I**, and so far accessible exclusively by milling. Selective synthesis and polymorph control were successfully scaled up to 10-g scale and to flow extrusion processing using different liquid additives and milling conditions. The activity of vitamin C was not deteriorated by mechanochemical stress or inclusion into a cocrystal, and the cocrystals showed excellent tableting properties. To the best of our knowledge, this is the first example of polymorphic control in a TSE process reported to date. Considering the importance and potential in the pharmaceutical industry that cocrystals gained recently, we believe that examples of large-scale production are necessary to help to implement mechanochemical procedures as green and sustainable manufacturing processes.

ASSOCIATED CONTENT

Supporting Information

The Supporting Information is available free of charge on the ACS Publications website at DOI: 10.1021/acssuschemeng.9b00043.

Additional PXRD, FTIR-ATR, Raman, and particle size distribution data (PDF)

AUTHOR INFORMATION

Corresponding Author

*E-mail: krunoslav.uzarevic@irb.hr.

ORCID

Tomislav Stolar: 0000-0002-9824-4462
Stipe Lukin: 0000-0003-2247-6803
Ivan Halasz: 0000-0002-5248-4217
Krunoslav Užarević: 0000-0002-7513-6485

Author Contributions

The manuscript was written by T.S., S.L., I.H., and K.U. All authors have given approval to the final version of the manuscript.

Notes

The authors declare no competing financial interest.

■ ACKNOWLEDGMENTS

S.L. is supported by the Croatian Science Foundation (Grant No. UIP-2014-09-4744). We are grateful to the staff of the 11-BM beamline for powder X-ray data collection. Use of the Advanced Photon Source at Argonne National Laboratory was supported by the U.S. Department of Energy, Office of Science, Office of Basic Energy Sciences, under Contract No. DE-AC02-06CH11357.

■ REFERENCES

(1) Do, J.-L.; Friščić, T. Mechanochemistry: A Force of Synthesis. *ACS Cent. Sci.* **2017**, *3*, 13−19.

(2) James, S. L.; Adams, C. J.; Bolm, C.; Braga, D.; Collier, P.; Friščić, T.; Grepioni, F.; Harris, K. D. M.; Hyett, G.; Jones, W.; et al. Mechanochemistry: opportunities for new and cleaner synthesis. *Chem. Soc. Rev.* **2012**, *41*, 413−447.

(3) Friščić, T. Supramolecular concepts and new techniques in mechanochemistry: cocrystals, cages, rotaxanes, open metal−organic frameworks. *Chem. Soc. Rev.* **2012**, *41*, 3493−3510.

(4) Baláž, P.; Achimovičová, M.; Baláž, M.; Billik, P.; Cherkezova-Zheleva, Z.; Criado, J. M.; Delogu, F.; Dutková, E.; Gaffet, E.; Gotor, F. J.; Kumar, R.; Mitov, I.; Rojac, T.; Senna, M.; Streletskii, A.; Wieczorek-Ciurowa, K. Hallmarks of mechanochemistry: from nanoparticles to technology. *Chem. Soc. Rev.* **2013**, *42*, 7571−7637.

(5) Roschangar, F.; Colberg, J.; Dunn, P. J.; Gallou, F.; Hayler, J. D.; Koenig, S. G.; Kopach, M. E.; Leahy, D. K.; Mergelsberg, I.; Tucker, J. L.; Sheldon, R. A.; Senanayake, C. H. A deeper shade of green: inspiring sustainable drug manufacturing. *Green Chem.* **2017**, *19*, 281−285.

(6) Friščić, T.; Jones, W. Recent Advances in Understanding the Mechanism of Cocrystal Formation via Grinding. *Cryst. Growth Des.* **2009**, *9*, 1621−1637.

(7) Hasa, D.; Jones, W. Screening for new pharmaceutical solid forms using mechanochemistry: A practical guide. *Adv. Drug Delivery Rev.* **2017**, *117*, 147−161.

(8) Braga, D.; Maini, L.; Grepioni, F. Mechanochemical preparation of co-crystals. *Chem. Soc. Rev.* **2013**, *42*, 7638−7648.

(9) Fleischman, S. G.; Kuduva, S. S.; McMahon, J. A.; Moulton, B.; Bailey Walsh, R. D.; Rodríguez-Hornedo, N.; Zaworotko, M. J. Crystal Engineering of the Composition of Pharmaceutical Phases: Multiple-Component Crystalline Solids Involving Carbamazepine. *Cryst. Growth Des.* **2003**, *3*, 909−919.

(10) Tan, D.; Loots, L.; Friščić, T. Towards medicinal mechanochemistry: evolution of milling from pharmaceutical solid form screening to the synthesis of active pharmaceutical ingredients (APIs). *Chem. Commun.* **2016**, *52*, 7760−7781.

(11) Colacino, E.; Porcheddu, A.; Halasz, I.; Charnay, C.; Delogu, F.; Guerra, R.; Fullenwarth, J. Mechanochemistry for "no solvent, no base" preparation of hydantoin-based active pharmaceutical ingredients: nitrofurantoin and dantrolene. *Green Chem.* **2018**, *20*, 2973−2977.

(12) Andre, V.; Hardeman, A.; Halasz, I.; Stein, R. S.; Jackson, G. J.; Reid, D. G.; Duer, M. J.; Curfs, C.; Duarte, M. T.; Friščić, T. Mechanosynthesis of the Metallodrug Bismuth Subsalicylate from Bi_2O_3 and Structure of Bismuth Salicylate without Auxiliary Organic Ligands. *Angew. Chem.* **2011**, *123*, 8004−8007.

(13) Crawford, D. E.; Casaban, J. Recent Developments in Mechanochemical Materials Synthesis by Extrusion. *Adv. Mater.* **2016**, *28*, 5747−5754.

(14) Crawford, D. E.; Miskimmin, C. K. G.; Albadarin, A. B.; Walker, G.; James, S. L. Organic synthesis by Twin Screw Extrusion (TSE): continuous, scalable and solvent-free. *Green Chem.* **2017**, *19*, 1507−1518.

(15) Cao, Q.; Howard, J. L.; Crawford, D. E.; James, S. L.; Browne, D. L. Translating solid state organic synthesis from a mixer mill to a continuous twin screw extruder. *Green Chem.* **2018**, *20*, 4443−4447.

(16) Ardila-Fierro, K. J.; Crawford, D. E.; Körner, A.; James, S. L.; Bolm, C.; Hernández, J. G. Papain-catalysed mechanochemical synthesis of oligopeptides by milling and twin-screw extrusion: application in the Juliá−Colonna enantioselective epoxidation. *Green Chem.* **2018**, *20*, 1262−1269.

(17) Crawford, D. E.; Casaban, J.; Haydon, R.; Giri, N.; McNally, T.; James, S. L. Synthesis by extrusion: continuous, large-scale preparation of MOFs using little or no solvent. *Chem. Sci.* **2015**, *6*, 1645−1649.

(18) Karadeniz, B.; Howarth, A. J.; Stolar, T.; Islamoglu, T.; Dejanović, I.; Tireli, M.; Wasson, M. C.; Moon, S.-Y.; Farha, O. K.; Friščić, T.; Užarević, K. Benign by Design: Green and Scalable Synthesis of Zirconium UiO-Metal−Organic Frameworks by Water-Assisted Mechanochemistry. *ACS Sustainable Chem. Eng.* **2018**, *6*, 15841−15849.

(19) Crawford, D. E.; James, S. L.; McNally, T. Use of Batch Mixing To Investigate the Continuous Solvent-Free Mechanical Synthesis of OLED Materials by Twin-Screw Extrusion (TSE). *ACS Sustainable Chem. Eng.* **2018**, *6*, 193−201.

(20) Daurio, D.; Nagapudi, K.; Li, L.; Quan, P.; Nunez, F.-A. Application of twin screw extrusion to the manufacture of cocrystals: scale-up of AMG 517−sorbic acid cocrystal production. *Faraday Discuss.* **2014**, *170*, 235−249.

(21) Daurio, D.; Medina, C.; Saw, R.; Nagapudi, K.; Alvarez-Núñez, F. Application of Twin Screw Extrusion in the Manufacture of Cocrystals, Part I: Four Case Studies. *Pharmaceutics* **2011**, *3*, 582−600.

(22) Medina, C.; Daurio, D.; Nagapudi, K.; Alvarez-Núñez, F. Manufacture of pharmaceutical co crystals using twin screw extrusion: A solvent less and scalable process. *J. Pharm. Sci.* **2010**, *99*, 1693−1696.

(23) Trask, A. V.; Motherwell, W. D. S.; Jones, W. Pharmaceutical Cocrystallization: Engineering a Remedy for Caffeine Hydration. *Cryst. Growth Des.* **2005**, *5*, 1013−1021.

(24) Trask, A. V.; Motherwell, W. D. S.; Jones, W. Physical stability enhancement of theophylline via cocrystallization. *Int. J. Pharm.* **2006**, *320*, 114−123.

(25) Jones, W.; Motherwell, W.; Trask, A. V. Pharmaceutical Cocrystals: An Emerging Approach to Physical Property Enhancement. *MRS Bull.* **2006**, *31*, 875−879.

(26) Karki, S.; Friščić, T.; Fábián, L.; Laity, P. R.; Day, G. M.; Jones, W. Improving Mechanical Properties of Crystalline Solids by Cocrystal Formation: New Compressible Forms of Paracetamol. *Adv. Mater.* **2009**, *21*, 3905−3909.

(27) Shiraki, K.; Takata, N.; Takano, R.; Hayashi, Y.; Terada, K. Dissolution improvement and the mechanism of the improvement from cocrystallization of poorly water-soluble compounds. *Pharm. Res.* **2008**, *25*, 2581−2592.

(28) McNamara, D. P.; Childs, S. L.; Giordano, J.; Iarriccio, A.; Cassidy, J.; Shet, M. S.; Mannion, R.; O'Donnell, E.; Park, A. Use of a Glutaric Acid Cocrystal to Improve Oral Bioavailability of a Low Solubility API. *Pharm. Res.* **2006**, *23*, 1888−1897.

(29) Good, D. J.; Rodríguez-Hornedo, N. Solubility Advantage of Pharmaceutical Cocrystals. *Cryst. Growth Des.* **2009**, *9*, 2252−2264.

(30) Babu, N. J.; Nangia, A. Solubility Advantage of Amorphous Drugs and Pharmaceutical Cocrystals. *Cryst. Growth Des.* **2011**, *11*, 2662−2679.

(31) Duggirala, N. K.; Perry, M. L.; Almarsson, Ö.; Zaworotko, M. J. Pharmaceutical cocrystals: along the path to improved medicines. *Chem. Commun.* **2016**, *52*, 640−655.

(32) Blagden, N.; Coles, S. J.; Berry, D. J. Pharmaceutical co-crystals − are we there yet? *CrystEngComm* **2014**, *16*, 5753−5761.

(33) Ross, S. A.; Lamprou, D. A.; Douroumis, D. Engineering and manufacturing of pharmaceutical co-crystals: a review of solvent-free manufacturing technologies. *Chem. Commun.* **2016**, *52*, 8772−8786.

(34) U.S. Department of Health and Human Services, Food and Drug Administration, Center for Drug Evaluation and Research (CDER). Regulatory Classification of Pharmaceutical Co-Crystals: Guidance for Industry, February 2018. https://www.fda.gov/downloads/Drugs/Guidances/UCM281764.pdf.

(35) http://www.entresto.com/index.jsp

(36) Pappenberger, G.; Hohmann, H.-P. Industrial production of L-ascorbic Acid (vitamin C) and D-isoascorbic acid. *Adv. Biochem. Eng./Biotechnol.* **2013**, *143*, 143−188.
(37) https://www.accessdata.fda.gov/scripts/cdrh/cfdocs/cfcfr/CFRSearch.cfm?fr=172.315 (accessed 22/02/2019).
(38) Buu-Hoï, N. P.; Ratsimamanga, A. R.; Xuong, N. D.; Nigeon-Dureuil, M. Study of nicastubine, an addition compound of vitamin PP and vitamin C. *Bull. Soc. Chim. Biol.* **1953**, *35*, 326−333.
(39) Stahly, G. P. A Survey of Cocrystals Reported Prior to 2000. *Cryst. Growth Des.* **2009**, *9*, 4212−4229.
(40) Bailey, C. W.; Bright, J. R.; Jasper, J. J. A Study of the Binary System Nicotinamide—Ascorbic Acid. *J. Am. Chem. Soc.* **1945**, *67*, 1184−1186.
(41) Fox, S. H.; Paterson, O. L. U.S. Patent US2433688A, 1943.
(42) Wenner, W. The reaction of *L*-ascorbic and *D*-isoascorbic acid with nicotinic acid and its amide. *J. Org. Chem.* **1949**, *14*, 22−26.
(43) Wang, J.-R.; Bao, J.; Fan, X.; Dai, W.; Mei, X. pH-Switchable vitamin B_9 gels for stoichiometry-controlled spherical co-crystallization. *Chem. Commun.* **2016**, *52*, 13452−13455.
(44) Friščić, T.; Halasz, I.; Beldon, P. J.; Belenguer, A. M.; Adams, F.; Kimber, S. A. J.; Honkimaki, V.; Dinnebier, R. E. Real-time and in situ monitoring of mechanochemical milling reactions. *Nat. Chem.* **2013**, *5*, 66−73.
(45) Halasz, I.; Puškarić, A.; Kimber, S. A. J.; Beldon, P. J.; Belenguer, A. M.; Adams, F.; Honkimäki, V.; Dinnebier, R. E.; Patel, B.; Jones, W.; Štrukil, V.; Friščić, T. Real Time In Situ Powder X ray Diffraction Monitoring of Mechanochemical Synthesis of Pharmaceutical Cocrystals. *Angew. Chem., Int. Ed.* **2013**, *52*, 11538−11541.
(46) Batzdorf, L.; Fischer, F.; Wilke, M.; Wenzel, K. J.; Emmerling, F. Direct In Situ Investigation of Milling Reactions Using Combined X ray Diffraction and Raman Spectroscopy. *Angew. Chem., Int. Ed.* **2015**, *54*, 1799−1802.
(47) Katsenis, A. D.; Puškarić, A.; Štrukil, V.; Mottillo, C.; Julien, P. A.; Užarević, K.; Pham, M.-H.; Do, T.-O.; Kimber, S. A. J.; Lazić, P.; Magdysyuk, O.; Dinnebier, R. E.; Halasz, I.; Friščić, T. *In situ* X-ray diffraction monitoring of a mechanochemical reaction reveals a unique topology metal-organic framework. *Nat. Commun.* **2015**, *6*, 6662.
(48) Užarević, K.; Halasz, I.; Friščić, T. Real-Time and In Situ Monitoring of Mechanochemical Reactions: A New Playground for All Chemists. *J. Phys. Chem. Lett.* **2015**, *6*, 4129−4140.
(49) Julien, P. A.; Užarević, K.; Katsenis, A. D.; Kimber, S. A. J.; Wang, T.; Farha, O. K.; Zhang, Y.; Casaban, J.; Germann, L. S.; Etter, M.; Dinnebier, R. E.; James, S. L.; Halasz, I.; Friščić, T. *In Situ* Monitoring and Mechanism of the Mechanochemical Formation of a Microporous MOF-74 Framework. *J. Am. Chem. Soc.* **2016**, *138*, 2929−2932.
(50) Michalchuk, A. A. L.; Tumanov, I. A.; Konar, S.; Kimber, S. A. J.; Pulham, C. R.; Boldyreva, E. V. Challenges of Mechanochemistry: Is In Situ Real Time Quantitative Phase Analysis Always Reliable? A Case Study of Organic Salt Formation. *Adv. Sci.* **2017**, *4*, 1700132.
(51) Kulla, H.; Haferkamp, S.; Akhmetova, I.; Röllig, M.; Maierhofer, C.; Rademann, K.; Emmerling, F. In Situ Investigations of Mechanochemical One Pot Syntheses. *Angew. Chem., Int. Ed.* **2018**, *57*, 5930−5933.
(52) Wilke, M.; Casati, N. Insight into the Mechanochemical Synthesis and Structural Evolution of Hybrid Organic−Inorganic Guanidinium Lead(II) Iodides. *Chem. - Eur. J.* **2018**, *24*, 17701.
(53) Stolar, T.; Batzdorf, L.; Lukin, S.; Žilić, D.; Motillo, C.; Friščić, T.; Emmerling, F.; Halasz, I.; Užarević, K. In Situ Monitoring of the Mechanosynthesis of the Archetypal Metal−Organic Framework HKUST-1: Effect of Liquid Additives on the Milling Reactivity. *Inorg. Chem.* **2017**, *56*, 6599−6608.
(54) Gracin, D.; Štrukil, V.; Friščić, T.; Halasz, I.; Užarević, K. Laboratory Real Time and In Situ Monitoring of Mechanochemical Milling Reactions by Raman Spectroscopy. *Angew. Chem., Int. Ed.* **2014**, *53*, 6193−6197.
(55) Kawashima, Y.; Imai, M.; Takeuchi, H.; Yamamoto, H.; Kamiya, K.; Hino, T. Improved flowability and compactibility of spherically agglomerated crystals of ascorbic acid for direct tableting designed by spherical crystallization process. *Powder Technol.* **2003**, *130*, 283−289.
(56) Urabe, M.; Ito, S.; Itai, S.; Yuasa, H.; Kanaya, Y. Assessment of tableting properties using infinitesimal quantities of powdered medicine. *Int. J. Pharm.* **2003**, *263*, 183−187.
(57) Urabe, M.; Ito, S.; Itai, S.; Yuasa, H. Assessment of tableting properties using infinitesimal quantities of powder medicine II. *J. Drug Delivery Sci. Technol.* **2006**, *16*, 357−361.
(58) Filimonova, A. V.; Tret'yakova, Y. A.; Gavrilov, A. S. 3D-modeling of the influence of isomalt, glucose, and compaction pressure on the quality of ascorbic-acid tablets. *Pharm. Chem. J.* **2018**, *52*, 467−472.
(59) Milardović, S.; Kereković, I.; Derrico, R.; Rumenjak, V. A novel method for flow injection analysis of total antioxidant capacity using enzymatically produced ABTS*+ and biamperometric detector containing interdigitated electrode. *Talanta* **2007**, *71*, 213−220.
(60) Lukin, S.; Stolar, T.; Tireli, M.; Blanco, M. V.; Babić, D.; Friščić, T.; Užarević, K.; Halasz, I. Tandem in Situ Monitoring for Quantitative Assessment of Mechanochemical Reactions Involving Structurally Unknown Phases. *Chem. - Eur. J.* **2017**, *23*, 13941−13949.
(61) Jaumot, J.; de Juan, J.; Tauler, R. MCR-ALS GUI 2.0: new features and applications. *Chemom. Intell. Lab. Syst.* **2015**, *140*, 1−12.
(62) de Juan, A.; Jaumot, J.; Tauler, R. Multivariate Curve Resolution (MCR). Solving the mixture analysis problem. *Anal. Methods* **2014**, *6*, 4964−4976.
(63) Shan, N.; Toda, F.; Jones, W. Mechanochemistry and co-crystal formation: effect of solvent on reaction kinetics. *Chem. Commun.* **2002**, *0*, 2372−2373.
(64) Trask, A. V.; Motherwell, W. D. S.; Jones, W. Solvent-drop grinding: green polymorph control of cocrystallisation. *Chem. Commun.* **2004**, *0*, 890−891.
(65) Friščić, T.; Trask, A. V.; Jones, W.; Motherwell, W. D. S. Screening for Inclusion Compounds and Systematic Construction of Three Component Solids by Liquid Assisted Grinding. *Angew. Chem., Int. Ed.* **2006**, *45*, 7546−7550.
(66) Hasa, D.; Miniussi, E.; Jones, W. Mechanochemical Synthesis of Multicomponent Crystals: One Liquid for One Polymorph? A Myth to Dispel. *Cryst. Growth Des.* **2016**, *16*, 4582−4588.
(67) Belenguer, A. M.; Lampronti, G. I.; De Mitri, N.; Driver, M.; Hunter, C. A.; Sanders, J. K. M. Understanding the influence of surface solvation and structure on polymorph stability: a combined mechanochemical and theoretical approach. *J. Am. Chem. Soc.* **2018**, *140*, 17051−17059.
(68) Etter, M. C.; MacDonald, J. C.; Bernstein, J. Graph-set analysis of hydrogen-bond patterns in organic crystals. *Acta Crystallogr., Sect. B: Struct. Sci.* **1990**, *B46*, 256−262.
(69) Bag, P. P.; Patni, M.; Malla Reddy, C. A kinetically controlled crystallization process for identifying new co-crystal forms: fast evaporation of solvent from solutions to dryness. *CrystEngComm* **2011**, *13*, 5650−5652.
(70) Ostwald, W. Studien über die Bildung und Umwandlung fester Körper. *Z. Phys. Chem.* **1897**, *22*, 289−330.
(71) Miller, N. J.; Rice-Evans, C.; Davies, M. J.; Gopinathan, V.; Milner, A. A Novel Method for Measuring Antioxidant Capacity and its Application to Monitoring the Antioxidant Status in Premature Neonates. *Clin. Sci.* **1993**, *84*, 407−412.
(72) Re, R.; Pellegrini, N.; Proteggente, A.; Pannala, A.; Yang, M.; Rice-Evans, C. Antioxidant activity applying an improved ABTS radical cation decolorization assay. *Free Radical Biol. Med.* **1999**, *26*, 1231−1237.
(73) Han, X.; Ghoroi, C.; To, D.; Chen, Y.; Davé, R. Simultaneous micronization and surface modification for improvement of flow and dissolution of drug particles. *Int. J. Pharm.* **2011**, *415*, 185−195.
(74) Bučar, D.-K.; Elliott, J. A.; Eddleston, M. D.; Cockcroft, J. K.; Jones, W. Sonocrystallization Yields Monoclinic Paracetamol with Significantly Improved Compaction Behavior. *Angew. Chem., Int. Ed.* **2015**, *54*, 249−253.

(75) Joiris, E.; Martino, P. D.; Berneron, C.; Guyot-Hermann, A.-M.; Guyot, J.-C. Compression Behavior of Orthorhombic Paracetamol. *Pharm. Res.* **1998**, *15*, 1122−1130.